Nuclear Materials and Energy 15 (2018) 190–194

Contents lists available at ScienceDirect

Nuclear Materials and Energy

journal homepage: www.elsevier.com/locate/nme

Corrosion characteristics of reduced activation ferritic-martensitic steel EUROFER by Li_2TiO_3 with excess Li

Keisuke Mukai[a,b,*], Fernando Sanchez[c], Tsuyoshi Hoshino[d], Regina Knitter[a]

[a] Institute for Applied Materials (IAM), Karlsruhe Institute of Technology, 76021 Karlsruhe, Germany
[b] Institute of Advanced Energy, Kyoto University, 611-0011 Uji, Japan
[c] National Fusion Laboratory, Division of Fusion Technology, CIEMAT, 28040 Madrid, Spain
[d] Fusion Energy Research and Development Directorate, National Institutes for Quantum and Radiological Science and Technology, 039-3212 Aomori, Japan

ARTICLE INFO

Keywords:
Corrosion
RAFM steel
Ceramic breeder
DEMO blanket
Compatibility

ABSTRACT

In a solid breeding blanket, ceramic breeder pebbles are in contact with reduced activation ferritic martensitic (RAFM) steel at high temperatures for years and accordingly form a corrosion layer on the blanket structural steel. Present study focuses on corrosion characteristics of EUROFER97 RAFM steel by an advanced breeder material of Li_2TiO_3 with excess Li (initial ratio of Li/Ti = 2.2) at 623, 823, and 1073 K under sweep gas (He + 0.1% H_2) flow. Formation of a thick oxide double layer was found on the surface of the EUROFER plates heated at 823 and 1073 K, while the corrosion layer formed at 673 K was < 1 μm even after 56 days. On the other hand, the changes that appeared on the contacted surface of the breeder pellet were insignificant. The growth of the corrosion layer shows that the corrosion caused by inward migrations mainly of Li and O from the breeder material will have little influence on mechanical property of the blanket structural steel.

1. Introduction

Reduced activation ferritic martensitic (RAFM) steel, such as F82H and EUROFER, have been intensively developed for advanced fission reactors and fusion applications. The compositions of EUROFER and F82H are in the range of Fe; 7.5–8.5% Cr; 1.0–2.0% W; 0.20–0.25% V; 0.04–0.08% Ta; 0.1% C for both high irradiation resistance and low activation characteristics [1]. The target temperatures of RAFM structural steel for water- and helium-cooled solid breeding blanket are 598 and 673–773 K, respectively [2]. Ceramic breeder pebbles are packed in the blanket for tritium production by nuclear transmutation of Li and used for years of operational period. Ternary oxides of Li_2TiO_3 (lithium metatitanate) and Li_4SiO_4 (lithium orthosilicate) are promising candidates for ceramic breeders, whereas advanced ceramic breeder materials are being studied to improve their performances. Two-phase material of Li_4SiO_4 with addition of 10–30 mol% Li_2TiO_3 has been developed in EU to increase the mechanical properties of the breeder pebbles [3], while maintaining its good capability of reprocessing [4,5]. Li_2TiO_3 with excess Li, with a Li_2O-rich composition in the non-stoichiometry range from 47 to 51.5 mol% TiO_2 [6], has been developed in Japan to be employed for a future DEMO blanket because high Li density is beneficial to tritium production [2,7].

Oxide corrosion layers reportedly form on stainless/RAFM steel by long-term contact with stoichiometric Li_2TiO_3 at high temperature and gradually grow with time [8,9] Our previous compatibility studies between EUROFER and Li_4SiO_4 with addition of 20 mol% Li_2TiO_3 indicated that the oxide double layer on the EUROFER plate, Fe-rich outer and Cr-rich inner layer, formed as a result of ionic migrations [10,11]. The obtained growth rates were parabolic in time in the temperature range of 623–1073 K. Corrosion characteristics of RAFM steel by Li_2TiO_3 with excess Li, however, has rarely been reported until today. As non-stoichiometric compounds with Li_2O-rich composition have been reported to show altered chemical behaviour at high temperature [12,13], the excess Li in Li_2TiO_3 may have an additional influence on the corrosion characteristics of RAFM steel.

This work aims to investigate the corrosion characteristics of EUROFER steel by Li_2TiO_3 with excess Li. EUROFER steel was contacted with Li_2TiO_3 with excess Li (initial Li/Ti ratio = 2.20) under sweep gas (He + 0.1%H_2) flow condition. The heating temperatures of 623 and 823 K were selected to be relevant for the temperatures of RAFM steel in the water- and helium-cooled DEMO blanket design. In addition, the specimens were heated at 1073 K for up to 28 days as an accelerated test. While there will be contact and non-contacted interfaces between breeder pebble and RAFM steel inside the blanket, this work focuses on the contacted areas, on which harsher corrosion takes place [10]. After the heating experiments, the breeder and EUROFER specimens were

* Corresponding author.
E-mail address: k-mukai@iae.kyoto-u.ac.jp (K. Mukai).

https://doi.org/10.1016/j.nme.2018.04.010
Received 29 November 2017; Received in revised form 29 March 2018; Accepted 19 April 2018
Available online 04 May 2018

analysed by scanning electron microscopy (SEM), energy dispersive X-ray microanalysis (EDX) and x-ray diffraction (XRD). Due to the poor scattering ability of X-ray by Li, secondary ion mass spectrometry (SIMS) was employed to examine element depth profile. The evolution of the corrosion layer and its rate-controlling step were investigated by analysing EUROFER specimens heated for five different periods at each temperature.

2. Method

Lithium metatitanate with excess Li was synthesized by the method proposed by Hoshino et al. [12] LiOH−H_2O (Alfa Aesar 99.995%) and H_2TiO_3 (Mitsuwa Chemicals Co., Ltd.) powders were mixed in a polyethylene bottle with a ratio of Li/Ti = 2.2. The bottle was rotated at 323 K to enhance dehydration reaction between the starting materials. After the rotation for 24 h, a dehydrated slurry was obtained. The slurry was dried at 623 K and then calcined at 923 K for 5 h in air. The calcined powder was shaped into a pellet with a diameter of 8 mm and heated at 1473 K for 2 h in H_2 atmosphere. The height and the sintering densities of the pellets were 3 mm and 83–85%T.D. respectively.

Heating experiment was carried out in alumina containers inside an atmosphere controllable tube furnace [10]. In the container, the pellet of Li_2TiO_3 with excess Li was sandwiched between two EUROFER 97 plates (11 mmϕ × 5 mmh) by using an Inconel spring. Five of the alumina containers were put in an alumina tube and heated with a flow gas of He + 0.1% H_2 with the constant flow rate of 1200 ml/min. These five containers were extracted after 3, 7, 14, 21, and 28 days in the heating experiment at 823 and 1073 K. On the other hand, longer heating periods (7, 14, 28, 56, and 84 days) were applied to the heating experiment at 623 K. During the sample extraction, the temperature of the furnace was temporary cooled down to 573 K. By using the electric pressure controller (EL-PRESS by Bronkhorst), pressure in the alumina tube was controlled to be at a positive pressure of 1.2 bar to keep air from flowing into the tube.

After the heating experiments, surface XRD analysis was performed with a Bruker D8 using Cu–Kα radiation by collecting diffraction data in the 2θ range from 15 to 70°. The polished surface of the EUROFER plate before the heating test exhibited a diffraction pattern of ferritic steel (α-Fe) body-centered-cubic (bcc) structure. It is noted that the heating temperature of 1073 K is lower than the ferrite-austenite (α–γ) transformation temperature of EUROFER97, which is reported to be 1099 K for an infinitely slow heating rate [14]. Cross-sections were studied by scanning electron microscopy (SEM SUPRA 55 by Zeiss) with an angle selective backscatter (AsB) detector to visualize a compositional contrast. Element distributions were investigated by energy dispersive X-ray microanalysis (EDX, Genesis XM2, Apollo 40 detector). The EUROFER specimens of 623 and 823 K, which were heated for 54 and 3 days respectively, were chosen for SIMS measurement. The EUROFER specimens were sputtered by oxygen primary ion using the ion source (IG-20 by Hiden) and then analysed by the quadrupole mass analyser (MAXIM HAL 7 by Hiden). A constant sputtering rate of 0.20 ± 0.03 nm/s was obtained from depth measurement of ion eroded crater after the SIMS measurements by using Bruker Dektak XT profilemeter.

3. Results and discussion

During heating the alumina container with the specimens, the average moisture concentrations of the outlet gas at 623, 823, and 1073 K were 0.016, 0.017, and 0.010 vol.% with variation of 0.003 vol.%. No trend in moisture concentration was observed during the experiment. The average moisture concentration of the inlet gas was < 0.003 vol.%. The difference of humidity between the inlet and the outlet gas is mainly attributed to water release from the breeder pellets. Gas supply into the alumina tube was interrupted after 25 days during the heating test at 823 K. The shortage of gas flow resulted in a loss of the positive pressure and a significant increase of the H_2O concentration up to 0.126 vol.%, thus the specimen after 28 days was not investigated in this study.

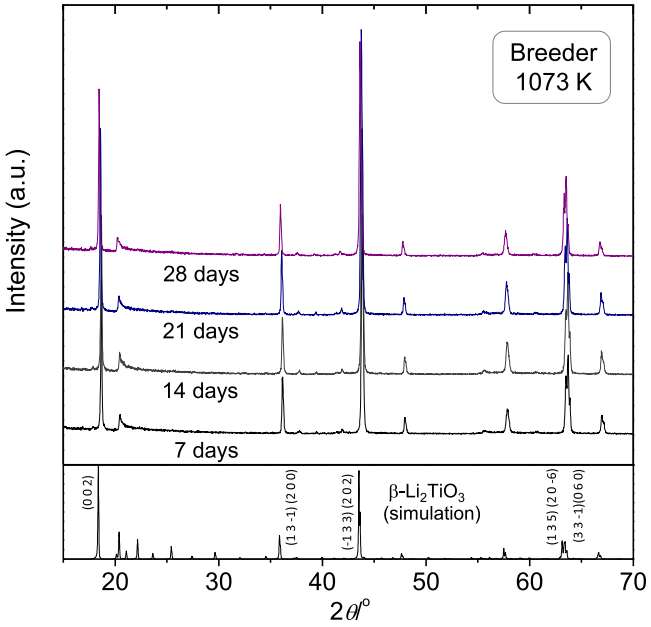

Fig. 1. XRD patterns from the breeder pellets heated at 1073 K for 1–4 weeks with simulation pattern of β-Li_2TiO_3.

Fig. 1 shows XRD patterns from the breeder pellets heated at 1073 K. The diffraction patterns were indexed by monoclinic β-Li_2TiO_3 (2C/c) phase [15]. No impurity peak or phase separation was found from the data of 1073 K as well as those of 623 and 823 K (data not shown). Rietveld analysis was performed on the XRD data from the breeder pellets, as a loss of the constituent elements such as Li and O may alter cell size of the monoclinic crystal. But, the changes in the refined lattice constants were within experimental error at all the heating temperatures. The monoclinic crystal structure is expected to be maintained by the formation of Li-deficient solid solutions (TiO_2 > 50 mol%) within the homogeneity range of this range.

The EUROFER plates after heating at 623 K represented an oxidized surface in the contact area with the breeder pellet, while uncontacted areas maintained their metallic surface. On the other hand, oxidized surfaces without metallic luster were observed for the EUROFER pellets heated at 823 and 1073 K. Cross-section SEM images of the EUROFER plates in contact with the breeder pellet after heating at 623 K and 823 K are summarized in Fig. 2. The formation of a corrosion layer was not found on the cross-section of the EUROFER plate heated at 623 K even after 84 days (Fig. 1a), though some oxide particles were observed on the surface. On the other hand, the EUROFER plates heated at 823 K (Fig. 2b–d) showed the formation of corrosion layers, which grew gradually up to 6.5 ± 0.8 μm after 21 days. Fig. 3 shows SIMS depth profiles from the EUROFER plate heated at 623 K after 56 days and at 823 K for 3 days. The profiles show that an oxidized layer formed on the EUROFER plate at 623 K as well as at 823 K. The oxide had two distinguishable layers. The outer oxide layer contained an enriched content of Fe, while the Cr content was significantly lowered. On the other hand, Cr is segregated in the inner oxide layer. Inward migrations of Li, Ti and O from the breeder pellet into the EUROFER plate were found; but the migrating amount of Ti should be limited, because Ti is not a mobile element in general. The thicknesses of the oxidized layers in Fig. 3a and b are approximately 0.4 and 1.8 μm, respectively. It is noted that the thickness of the corrosion layer at 673 K was much thinner than in the previous study using breeder pellets of Li_4SiO_4 + 20 mol% Li_2TiO_3, where the thickness was 3.5 μm after heating in the same condition [10]. This indicates that Li_2TiO_3 with excess Li has a good

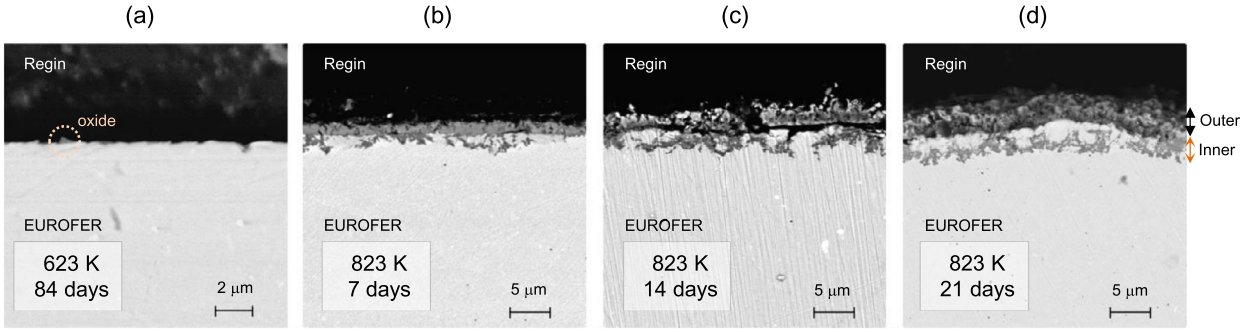

Fig. 2. Cross-section images of the EUROFER plates heated at 623 K for 84 days (a), at 823 K for 7 days (b), 14 days (c), and 21 days (d).

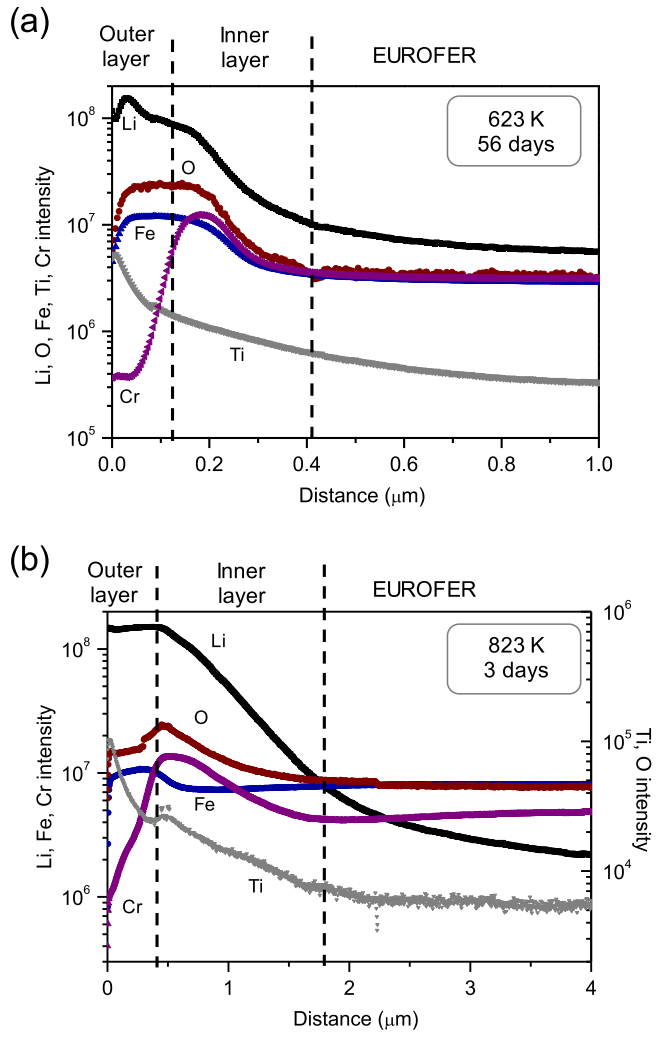

Fig. 3. SIMS depth profiles of EUROFER plates heated at 623 K for 56 days (a) and at 823 K for 3 days (b).

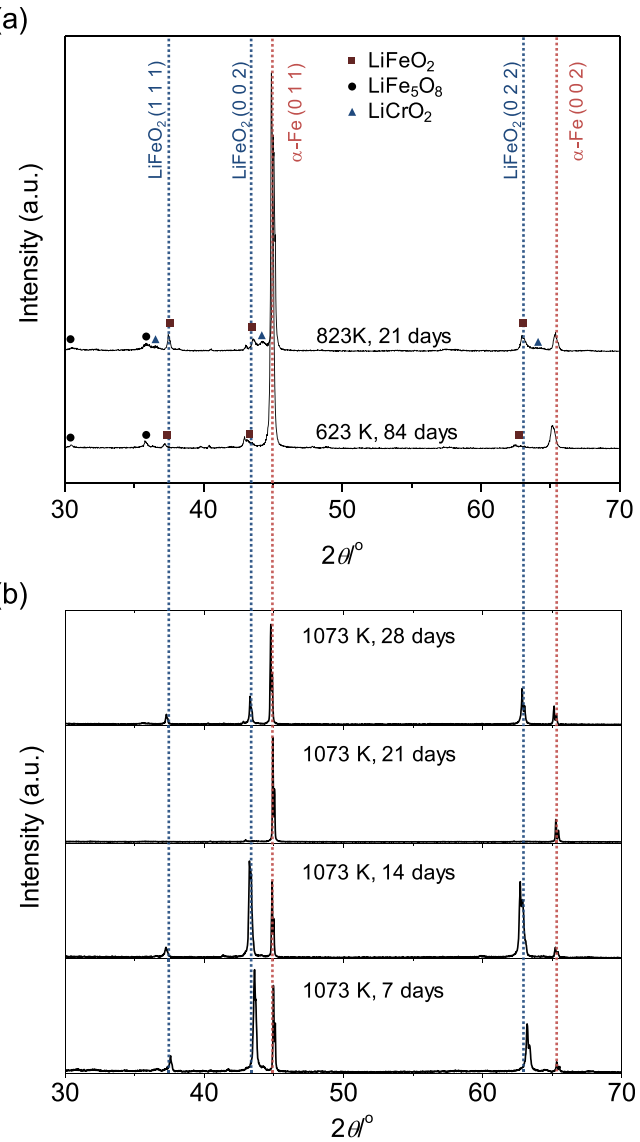

Fig. 4. XRD patterns of the EUROFER plates heated at 623 K, 823 K (a), and 1073 K (b).

compatibility with RAFM blanket steel at an operational temperature of the water-cooled blanket. Fig. 4 summarizes XRD patterns from the EUROFER plates. The pattern from the EUROFER at 623 and 823 K (Fig. 4a) exhibit peaks of $LiFe_5O_8$ ($Fd\bar{3}m$) and $LiFeO_2$ ($Fm\bar{3}m$) phase in addition to α-Fe peak, consistent with the element distribution in the outer layer established by SIMS.

Cross-section SEM images and EDX element mappings of the EUROFER heated at 1073 K are displayed in Fig. 5. Corrosion layers on the EUROFER plates heated at 1073 K for up to 14 days exhibited the formation of the double oxide layer, as displayed in Fig. 5a. The thicknesses of the oxide layers after 3, 7, and 14 days were 6.6 + 1.4, 11.7 ± 1.9, and 18.3 ± 0.9 μm. The XRD patterns from the EUROFER plates after 7 and 14 days (Fig. 4b) were α-Fe and $LiFeO_2$. It indicates that the outer layers of the specimens are $LiFeO_2$ phase. After 21 days, however, a metallic surface was observed as seen in Fig. 5b, while the Cr-rich inner oxide layer was maintained. The XRD pattern consistently

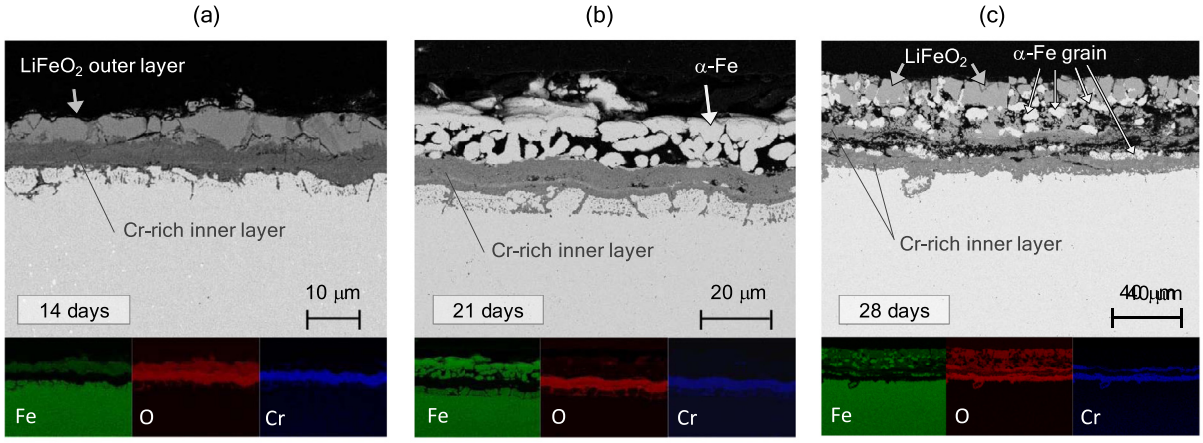

Fig. 5. SEM cross-section images and EDX element mappings on the EUROFER plates heated at 1073 K for 14 days (a), 21 days (b), and 28 days (c).

showed pattern of α-Fe metal, while diffraction peaks of $LiFeO_2$ were hardly detected. After 28 days, outer Fe-rich and inner Cr-rich oxide layers were observed with α-Fe grains distributed in both layers (Fig. 5c). The XRD pattern of the EUROFER after 28 days showed two-phase pattern of α-Fe and $LiFeO_2$. A rapid growth of the corrosion layer was seen after the reduction-oxidation event on the surface; the thickness of oxidized layer of the EUROFER surface after 21 and 28 days was 30.6 ± 2.6 and 42 ± 2.5 μm, respectively.

It is common behavior in oxidation of Fe–Cr alloy to form a hematite outer layer and a Cr-rich spinel inner layer. The lithiated corrosion layers observed in present study can be explained by oxidation and the following inward Li^+ diffusion into the oxidized layers. The thickness of the oxidized layer of the EUROFER surface, determined by oxygen mapping of EDX, is plotted in Fig. 6. The growth rate of the corrosion layer at 823 K was reduced with the heating period, and the data were fitted by a parabolic curve from the origin. This implies, by assuming the Wagner's hypotheses [16], that the growth rate is controlled by diffusion through the growing oxide layers. In the present work, the oxygen diffusion through the outer and/or the inner layer is supposed to be the rate-determining process. The parabolic curve yielded an effective diffusion coefficient of oxygen of 2.4×10^{-12} cm^2/s. The data at 1073 K after 3, 7, and 14 days also showed a parabolic growth (solid line). This curve gives an effective diffusion coefficient of 2.6×10^{-11} cm^2/s. However, the data after 21 days, where the metallic surface appeared in the outer layer, showed a sudden increase, termed breakaway oxidation, with a linear growth rate. It is implicit that the corrosion mechanism is changed from the ionic migration to reaction at the metallic surface after the breakaway event. The linear increase was caused by the oxidation of metallic grains rather than cracking or spalling off, because the protective Cr-rich inner layers remained in the EUROFER specimens (see Fig. 5).

In Fig. 7, effective diffusion coefficients at 823 K (until 21 days) and 1073 K (until 14 days) are plotted in an Arrhenius plot. The effective diffusion coefficients obtained in this study are comparable with the previous compatibility study between EUROFER and Li_4SiO_4 + 20 mol % Li_2TiO_3 [10]. Data at 673 K in the present study was not plotted in Fig. 7, because no corrosion layer was observed by SEM/EDX. But the effective diffusion coefficient at 673 K would be smaller than the effective diffusion coefficient of Li_4SiO_4 + 20 mol% Li_2TiO_3 at 673 K (1.6×10^{-14} cm^2/s). The Arrhenius equation, the slope of the dotted line in Fig. 7, yielded an activation energy of approximately 1.0 eV, in accordance with the previous result (0.93 eV). Given that the growth of the corrosion layer is controlled by ionic migration without a breakaway event during a two-year operation, the thickness of the corrosion

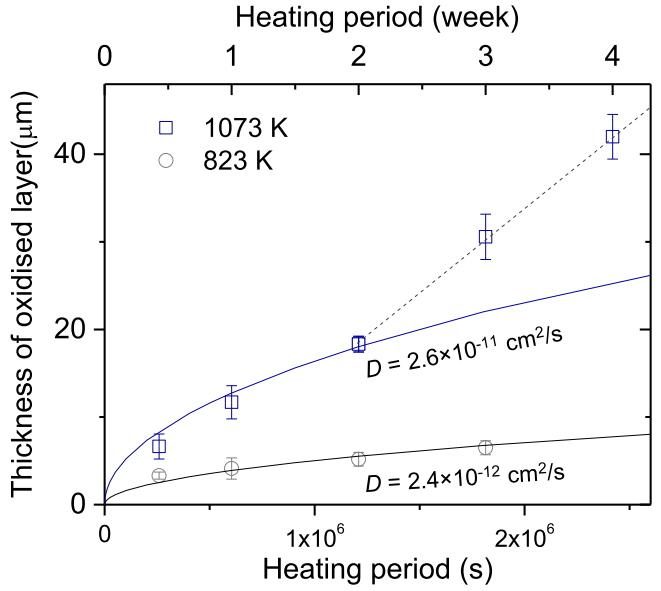

Fig. 6. Thickness of the corrosion layers on the EUROFER plates heated at 823 and 1073 K with effective diffusion coefficients of oxygen *D*.

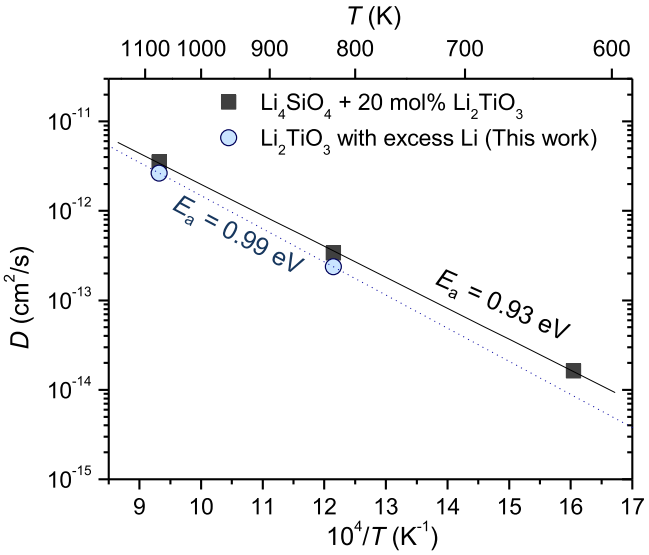

Fig. 7. Arrhenius plot of effective oxygen diffusion coefficient in comparison with the previous study using EUROFER97 and the two-phase ceramic breeder (Li_4SiO_4 + 20 mol% Li_2TiO_3) [10].

layer on the blanket structural steel will be less than 10 μm, based on the previous prediction [10]. Even if the contact area between blanket steel and ceramic breeder pebbles were heated up to 773 K, namely the maximum temperature of RAFM steel in the helium-cooled blanket concept [2], the fitting line in Fig. 7 (dotted line) predicts that the thickness after 2 years would only be 28 μm. As the thickness of the blanket structural steel is designed in the order of millimeters, the corrosion layer by Li_2TiO_3 with excess Li will not have a significant influence on mechanical property of blanket structural steel.

4. Conclusion

In this work, corrosion characteristics of EUROFER, a reduced activation ferritic martensitic (RAFM) steel, by Li_2TiO_3 with excess Li (initial Li/Ti ratio of 2.2) was studied at 623, 823, and 1073 K under sweep gas flow of He + 0.1% H_2. After the heating experiment, no significant change in the breeder specimens was found. On the other hand, the formation of a corrosion double layer, $LiFeO_2$ outer and Cr-rich inner layer, was observed at the surface of the EUROFER specimens in contact with the breeder pellet. The EUROFER plate was limitedly corroded at 623 K; the thickness of the corrosion layer was < 1 μm even after 56 days. The growth rates at 823 and 1073 K were parabolic until 14 days and 21 days, respectively. A breakaway caused by reduction and oxidation of the outer layer changed the rate-determining process and resulted in a linear increase of the thickness with time. But the corrosion by Li_2TiO_3 with excess Li will not cause a significant impact on the mechanical strength of the blanket structural steel because of the good chemical compatibility at blanket relevant temperatures.

Acknowledgments

This work has been carried out within the framework of the EUROfusion Consortium and has received funding from the Euratom research and training programme 2014–2018 under grant agreement No. 633053. The views and opinions expressed herein do not necessarily reflect those of the European Commission. The first author was supported by Japan Society for the Promotion of Science (JSPS) Overseas Research Fellowships.

References

[1] R.L. Klueh, A.T. Nelson, J. Nucl. Mat. 371 (2007) 37–52.
[2] S. Konishi, M. Enoeda, M. Nakamichi, T. Hoshino, A. Ying, S. Sharafat, S. Smolentsev, Nucl. Fusion 57 (2017) 092014.
[3] R. Knitter, M.H.H. Kolb, U. Kaufmann, A.A. Goraieb, J. Nucl. Mater. 442 (2013) S433–S436.
[4] K. Mukai, P. Pereslavtsev, U. Fischer, R. Knitter, Fusion Eng. Des. 100 (2015) 565–570.
[5] O. Leys, T. Bergfeldt, M.H.H. Kolb, R. Knitter, A.A. Goraieb, Fusion Eng. Des. 107 (2016) 70–74.
[6] H. Kleykamp, Fusion Eng. Des. 61 (2002) 361–366.
[7] T. Hoshino, Y. Edao, Y. Kawamura, K. Ochiai, Fusion Eng. Des. 109 (2016) 1114–1118.
[8] P.A. Finn, K. Kurasawa, S. Nasu, K. Noda, T. Takahashi, H. Takeshita, T. Tanifuji, H. Watanabe, Proceedings of IEEE Ninth Symposium on Engineering Problems of Fusion Research, vol. II, 1981, p. 1200.
[9] S. Cho, Y.H. Park, Y.B. Chun, K.M. Min, M.Y. Ahn, S.C. Park, Y. Lee, Fusion Eng. Des. 124 (2017) 1052–1058.
[10] K. Mukai, F. Sanchez, R. Knitter, J. Nucl. Mater. 488 (2017) 196–203.
[11] K. Mukai, M. Gonzalez, R. Knitter, Fusion Eng. Des. 125 (2017) 154–159.
[12] T. Hoshino, M. Yasumoto, K. Tsuchiya, K. Hayashi, H. Nishimura, A. Suzuki, T. Terai, Fusion Eng. Des. 82 (2007) 2269–2273.
[13] T. Hoshino, K. Kato, Y. Natori, M. Nakamura, K. Sasaki, K. Hayashi, T. Terai, K. Tatenuma, Fusion Eng. Des. 84 (2009) 956–959.
[14] K.D. Zilnyk, V.B. Oliveira, H.R.Z. Sandim, A. Möslang, D. Raabe, J. Nucl. Mater. 462 (2015) 360–367.
[15] K. Kataoka, Y. Takahashi, N. Kijima, H. Nagai, J. Akimoto, Y. Idemoto, K.-I. Ohshima, Mater. Res. Bull. 44 (2009) 168–172.
[16] C. Wagner, Corrosion Sci. 9 (1969) 91.